Reduction to the pole as an inverse problem and its application to low-latitude anomalies

João B. C. Silva*

ABSTRACT

Traditionally, reduction to the pole has been accomplished either by space- or wavenumber-domain filtering. In the two-dimensional case, this procedure is stable regardless of the latitude, as long as the source strike is not parallel to the horizontal projection of the geomagnetic field. In the three-dimensional case, however, reduction-to-the-pole filtering is stable only at high magnetic latitudes. At latitudes lower than 15 degrees, it is of no practical use due to a sharply increasing instability toward the magnetic equator.

The three-dimensional instability of this filtering technique is demonstrated, and the reduction-to-the-pole problem is formulated in the context of a general linear inverse problem. As a result, stable solutions are found by using well-known stabilizing procedures developed for the inverse linear problem. The distribution of magnetization of an equivalent layer of doublets that reproduces the observed data is computed. The magnetic doublets are parallel to the magnetization direction

which is assumed constant throughout the sources. The magnetic field reduced to the pole is then obtained by changing the inclinations of the geomagnetic field and the doublets to 90 degrees and recalculating the total field.

The usefulness and limitations of the method at low magnetic latitudes are assessed using theoretical data. The effects of noise and anomaly truncation are also investigated for both high and low latitudes. In all cases, application of the proposed method produced meaningful results regardless of the latitude.

The method is applied to field data from two different low-latitude anomalies. The first anomaly is due to a seamount in the Gulf of Guinea with reversed magnetization. The geomagnetic field at this location is about −23 degrees. The second anomaly is an intrabasement anomaly from Parnaiba Basin, Brazil, where the magnetization is assumed to be induced by a geomagnetic field with −1.4 degree inclination. The results obtained confirm that the proposed method produces stable, meaningful, reduced-to-the-pole maps.

INTRODUCTION

The reduction-to-the-pole technique was introduced by Baranov (1957) when he showed that the transformation is theoretically possible under the assumption that the magnetization vector is constant in all magnetized masses. Baranov's formulation requires numerical evaluation of a double integral which implies loss of accuracy. A procedure for the numerical calculation of the reduction-to-the-pole formula was given in Baranov and Naudy (1964). As they pointed out, when the inclination of the geomagnetic field is close to zero, structures in the north-south direction do not produce any anomaly except at their extremities. In this case, to obtain a reasonable reduction to the pole, it is necessary to have coefficients with high values, covering a large integration domain. However, the high-value coefficients also operate upon the noise so that noise enhancement is expected and the problem of reduction to the pole at low magnetic latitudes may be considered an unstable problem.

Bhattacharyya (1965) presented an improvement to Baranov's approach. The magnetic field is expanded in double Fourier series on a rectangular grid. The double integration then can be made analytically instead of numerically. However, the basic problem of instability at low latitudes remains. Moreover, calculations of the double Fourier series coefficients and of the field reduced to the pole require evaluation of many trigonometric functions. As pointed out in Ervin (1976), if only four coefficients for each harmonic are calculated simultaneously, the reduction to the pole of a 100 × 100 array requires evaluation of 105 000 000 trigonometric functions, but this figure can be substantially reduced by means of look-up tables (Ervin, 1976).

Kanasewich and Agarwal (1970) modified Bhattacharyya's method to take advantage of the fast Fourier transform algorithm, and Gunn (1975) showed that reduction to the pole is a linear transformation applied to the original field either in the space or wavenumber domain. In this respect, reduction to the pole can be viewed as a filtering operation. A better insight in

the reduction-to-the-pole process was possible then by investigating the properties of the reduction-to-the-pole filter in the wavenumber domain. However, the problem of numerical instability at low magnetic latitudes was not addressed in Gunn's paper.

Pearson and Skinner (1982) suggested a reduction-to-the-pole procedure in the wavenumber domain which operates on the spectrum of the data previously smoothed by a user-defined whitening factor. The aim of this whitening factor is to attenuate the noise content in the original data so that noise distortion in the reduced field is minimized. This approach is an attempt to deal with the instability of the reduction-to-the-pole procedure at low magnetic latitudes. However, applying the remedy to the data and not to the method presents some disadvantages. First, a priori information about the noise is needed to define the whitening factor. Also, noise elimination by spectral techniques is always imperfect. As a result, part of the noise remains in the filtered data, and is, therefore, enhanced since the method (of reducing the anomaly to the pole) is still unstable at low latitudes.

An entirely different approach based on equivalent sources has been adopted by some authors (Bott and Ingles, 1972; Emilia, 1973, for example). It consists of finding equivalent sources which, under the assumption of constant magnetization direction, explain the observed data. In a second stage the magnetic field reduced to the pole is obtained by recomputing the magnetic field due to the equivalent sources with the inclination of the geomagnetic field and of the magnetic moments set to 90 degrees. These authors used two-dimensional (2-D) sources and analyzed the magnetic field along profiles perpendicular to the source strike. Unless the 2-D structure is in the direction of the horizontal projection of the geomagnetic field or the magnetization, the 2-D reduction to the pole is a stable transformation. None of these authors

dipole spacing. However, as pointed out in Langel et al. (1984), published results using Mayhew's technique (Mayhew, 1982; Mayhew et al., 1980, for example) have all been at mid-latitudes. Close to the geomagnetic equator, extreme instability occurs in the magnetization solution. Langel et al. (1984) investigated the problem of instability in the solution of equivalent sources at low magnetic latitudes and used the technique of principal component regression to reduce instability. This technique essentially consists of eliminating the smallest singular values of a matrix that must be inverted to obtain the magnetization solution.

I demonstrate the instability of the reduction-to-the-pole filter at low magnetic latitudes and show that by formulating the problem of reduction to the pole as an inverse problem, stable solutions in the presence of noise can be found using well-known methods. These methods are given in Tikhonov and Arsenin (1977), and Hoerl and Kennard (1970a, b), for example. Consequently, meaningful results at low magnetic latitudes, where the instability is more pronounced, can be obtained. Initially, the magnetization of an equivalent layer of doublets is computed from the observed data. All magnetic doublets are assumed parallel to the magnetization vector whose direction is supposedly constant throughout the sources. Once the doublet strengths are found, the inclinations of the doublets and the geomagnetic field are changed to 90 degrees and the total magnetic field is recalculated. The first stage involves the solution of an inverse problem, while the second is a forward problem. Only the first stage presents instability so that a stabilizing procedure must be applied only there.

INSTABILITY OF REDUCTION-TO-THE-POLE FILTERING

In the wavenumber domain, the reduction-to-the-pole filter is given in (Gunn, 1975)

$$K(u, v) = \frac{1}{[iu \cos I_0 \cos D_0 + iv \cos I_0 \sin D_0 + (u^2 + v^2)^{1/2} \sin I_0][iu \cos I \cos D + iv \cos I \sin D + (u^2 + v^2)^{1/2} \sin I]}, \quad (1)$$

addressed the problem of 2-D reduction-to-the-pole instability at low magnetic latitudes.

von Frese et al. (1981) used equivalent dipole sources to perform differential reduction to the pole of satellite data where the dipole directions are assumed parallel to the local geomagnetic field. This technique has been applied at midlatitudes (von Frese et al., 1981; von Frese et al., 1982) and low latitudes (Hinze et al., 1982). Using a similar procedure, Mayhew (1979) inverted satellite data to find the magnetic moments of equivalent dipole sources. The smoothed, calculated field from this equivalent source was used as input to another model in which the sources were 2 degrees by 2 degrees spherical prisms. To minimize the usual numerical instability, the magnetic moments of the prisms were constrained to be specified by the coefficients in a double Fourier series in latitude and longitude. Mayhew (1982) analyzed the question of stability of dipole solution as a function of dipole spacing in degrees, and he concluded that 2.7 degrees is the optimum where $i = \sqrt{-1}$, and u and v are angular wavenumber coordinates. I and I_0 are the inclinations of the magnetization and the geomagnetic field, respectively, and D and D_0 are the azi-

muths of the magnetization vector and geomagnetic field with respect to the x-axis (these angles are positive). Notice that at $u = v = 0$, the filter operator is undefined. In other words, the base level value of the reduced-to-the-pole anomaly obtained by filtering is arbitrary.

The instability of this filter can be more easily seen in polar coordinates. Using the transformations $u = r \cos (\theta)$ and $v = r \sin (\theta)$, and after some manipulations, equation (1) becomes

$$K(r, \theta)$$
$$= \frac{1}{[i \cos I_0 \cos (D_0 - \theta) + \sin I_0][i \cos I \cos (D - \theta) + \sin I]}.$$
$$(2)$$

Equation (2) shows that close to the magnetic equator ($I_0 \simeq 0$ degrees) and for values of θ close to $D_0 \pm 90$ degrees, the imaginary and real parts of the complex filter weights are very high. In practice, this filter operates on the discrete spectrum of the original data, and this spectrum contains imperfections due to aliasing and Gibbs' phenomenon. Therefore, a poor performance of this filter can be expected at low mag-

netic latitudes even in the absence of noise because the imperfections in the spectrum will be enhanced by the large values of the filter weights along the direction $D_0 \pm 90$ degrees. Recall that the direction $D_0 \pm 90$ degrees in the wavenumber domain corresponds to the direction D_0 in space domain; a fictitious trend along D_0, due to filter enhancement of imperfections in this direction, is expected to show up when reducing low-latitude anomalies to the pole.

In 2-D problems this instability occurs only when the 2-D structure strike is close to the direction of the geomagnetic field or the magnetization. In three-dimensional (3-D) problems, however, the instability always occurs because there will always be a few points (u, v) in the 2-D data spectrum such that $\tan^{-1}(v/u)$ is close to the direction $D_0 \pm 90$ degrees.

To demonstrate the instability of the reduction-to-the-pole filter, I applied it to the magnetic field due to a vertical prism uniformly magnetized in the direction of the geomagnetic field (Bhattacharyya, 1964). In terms of grid units the prism is 2 units long (x-direction, assumed parallel to the north-south direction), 2 units wide (y-direction), and 4 units thick (z-direction). Its top is located 2 units below the plane of measurement and the magnetic susceptibility is 0.025 SI units. Figure 1 shows the plan view of the prism and the theoretical magnetic field at pole. Figures 2 and 3 show the map reduced to the pole using the fast Fourier transform (FFT) filtering technique described above, employing a 16×16 grid. In Figure 2 the original magnetic field is due to a prism with $I = I_0 = 10$ degrees and $D = D_0 = 20$ degrees, while in Figure 3 $I = I_0 = 5$ degrees and $D = D_0 = 20$ degrees was used. Both figures show that at an inclination of about 10 degrees the
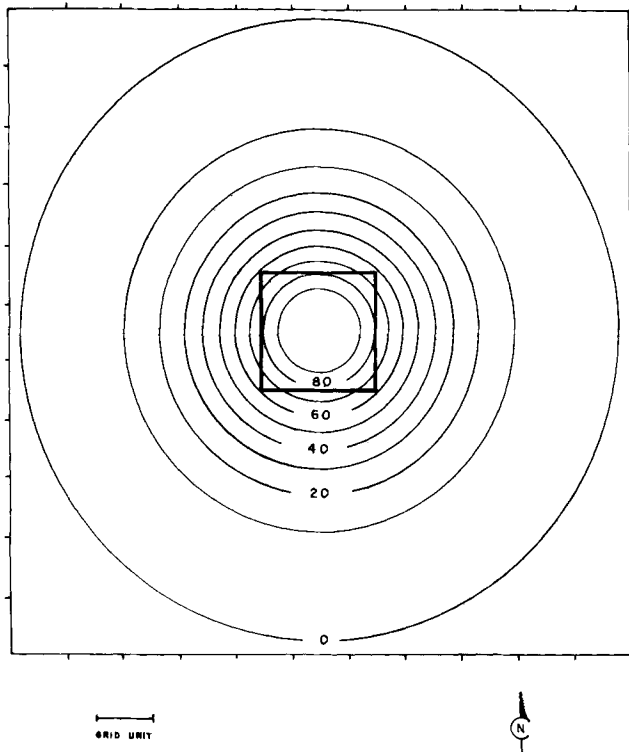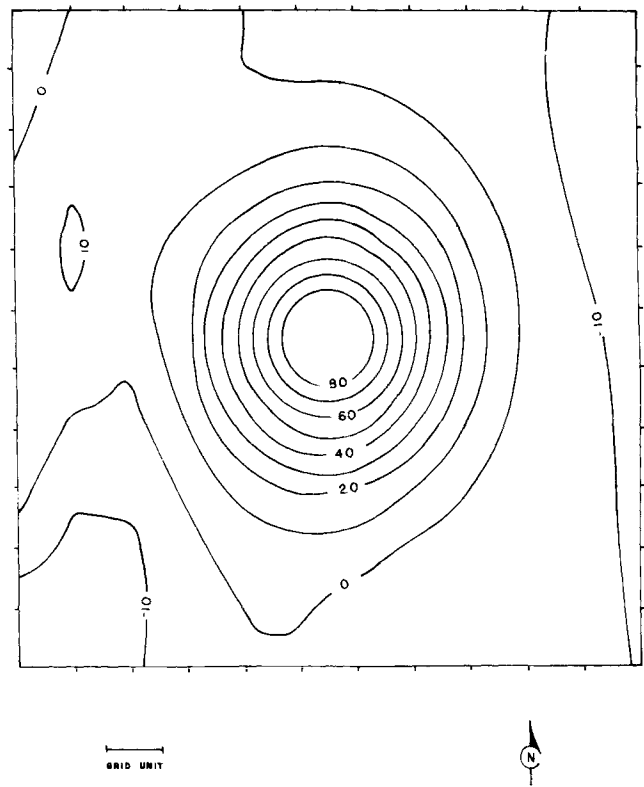

FIG. 2. Total field reduced to the pole using FFT filtering. $I = I_0 = 10$ degrees and $D = D_0 = 20$ degrees. Contour intervals: 10 nT.

FIG. 1. Plan view of the basic vertical prism and its theoretical total field anomaly at pole. Contour intervals: 10 nT.
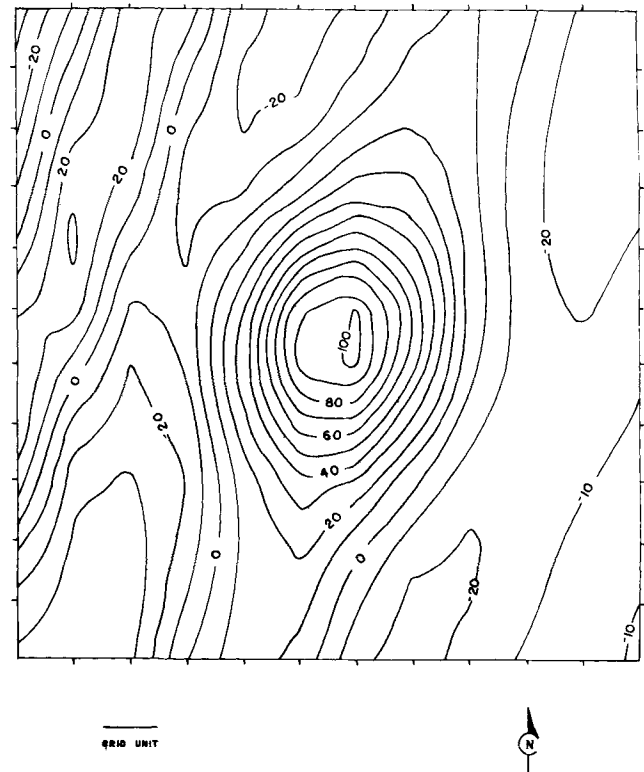

FIG. 3. Total field reduced to the pole using FFT filtering. $I = I_0 = 5$ degrees and $D = D_0 = 20$ degrees. Contour intervals: 10 nT.

filtering begins to yield poor results as compared to the theo-retical field of Figure 1. At an inclination of 5 degrees there is a severe distortion of the anomaly and a pronounced trend along 20 degrees northeast shows up, as predicted by the analysis of equation (2). As the inclination tends to zero, this trend becomes more distinct, squeezing the circular anomaly pattern into a straight line. At the same time, a profile normal to this direction shows oscillations whose amplitudes increase infinitely as the inclination approaches zero.

Because the original data are noise-free, the only way to reduce this instability is to obtain a more perfect repre-sentation of the data spectrum. To demonstrate this, the mag-netic field due to the same prism was computed in a 128×128 grid and the size of the area was doubled in both the x- and y-directions, keeping the prism at the center of the area. The absolute dimensions of the prism were maintained. The FFT filtering was applied to these data and the result is shown in Figure 4 for $I = I_0 = 5$ degrees and $D = D_0 = 20$ degrees. Comparison of Figures 3 and 4 shows that a distinct improve-ment occurs when a larger gridding area and a smaller grid interval are employed. However, in practice the data are ob-tained discretely so interpolation in a grid finer than the average original sampling spacing introduces spurious fre-quencies, i.e., noise. Moreover, an isolated anomaly seldom occurs, so it is rarely possible to extend the sampled area as desired without entering into the domain of interfering adja-cent anomalies.

In summary, the instability of the 3-D reduction-to-the-pole filter occurs at or near the magnetic equator because of the numerical pole presented by the filter at $I = 0$ degrees or $I_0 =$

0 degrees. This instability is very pronounced because of the presence of imperfections in the Fourier spectrum caused by aliasing and Gibbs' phenomenon.

REDUCTION TO THE POLE AS AN INVERSE PROBLEM

Let h_i^0 be the total magnetic field observed at point $P(x_i, y_i, z_i)$ referred to a right-handed Cartesian system of coordinates (Figure 5).

The magnetic field due to arbitrary sources can be exactly fitted by the magnetic field due to a horizontal equivalent layer of dipoles at depth $z = d$. For each depth there is a unique distribution of magnetization (dipole moment per unit surface) that fits the data (Roy, 1962). In practice, we have to simplify the problem and assume a discrete distribution of magnetization. I approximate the equivalent layer of dipoles by an equivalent layer of doublets at depth d. Each doublet has length b and is parallel to the unit magnetization vector $\hat{\alpha}$. The magnetization direction $\hat{\alpha}$ is assumed constant through-out the sources (Figure 6).

The magnetic field at point $P(x_i, y_i, z_i)$ due to the doublet centered at point $Q(x_j', y_j', d)$ (Figure 6) is

$$h_{ij} = a_{ij} \cdot p_j,$$

where p_j is the strength of the jth doublet, and

$$a_{ij} = \left[\frac{x_i - x_j' - \frac{b}{2} \cos I \cos D}{F_1} \right.$$
$$\left. - \frac{x_i - x_j' + \frac{b}{2} \cos I \cos D}{F_2} \right] \cos I_0 \cos D_0$$
$$+ \left[\frac{y_i - y_j' - \frac{b}{2} \cos I \sin D}{F_1} \right.$$
$$\left. - \frac{y_i - y_j' + \frac{b}{2} \cos I \sin D}{F_2} \right] \cos I_0 \sin D_0$$
$$+ \left[\frac{z_i - d - \frac{b}{2} \sin I}{F_1} - \frac{z_i - d + \frac{b}{2} \sin I}{F_2} \right] \sin I_0, \quad (3)$$
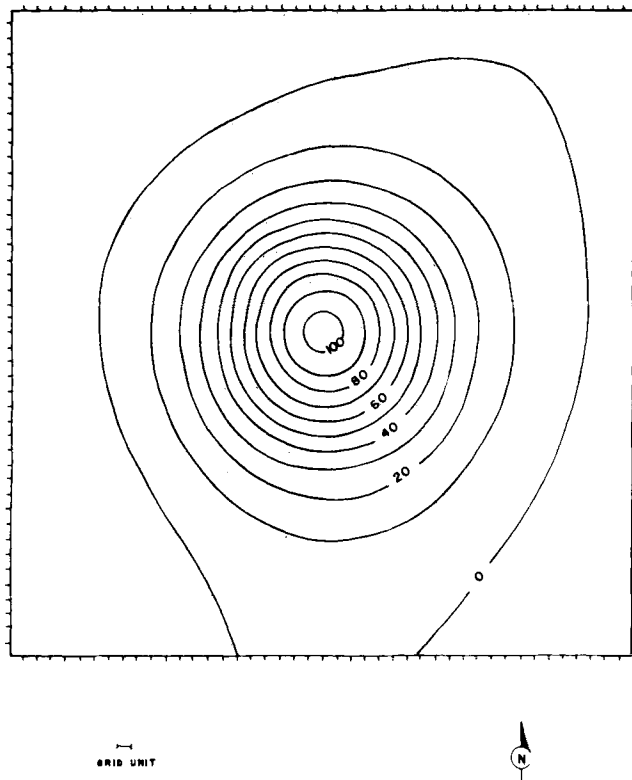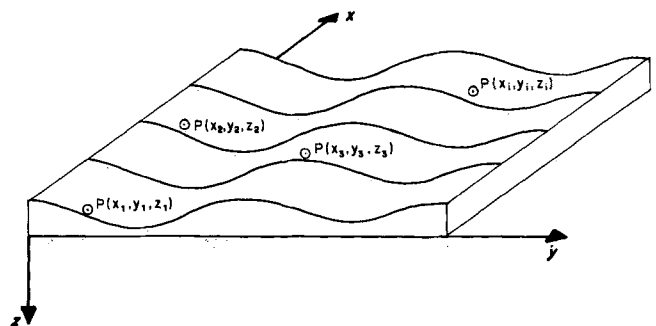
with

FIG. 4. Total field reduced to the pole using FFT filtering with a 128×128 grid. The figure shows the central part of the grid only. $I = I_0 = 5$ degrees and $D = D_0 = 20$ degrees. Contour intervals: 10 nT.

FIG. 5. Reference system employed for observations.

$$F_1 = \left[\left(x_i - x_j' - \frac{b}{2}\cos I \cos D\right)^2\right.$$

$$+ \left(y_i - y_j' - \frac{b}{2}\cos I \sin D\right)^2$$

$$\left. + \left(z_i - d - \frac{b}{2}\sin I\right)^2\right]^{3/2},$$

and

$$F_2 = \left[\left(x_i - x_j' + \frac{b}{2}\cos I \cos D\right)^2\right.$$

$$+ \left(y_i - y_j' + \frac{b}{2}\cos I \sin D\right)^2$$

$$\left. + \left(z_i - d + \frac{b}{2}\sin I\right)^2\right]^{3/2}$$

The total magnetic field h_i at point $P(x_i, y_i, z_i)$ due to all doublets is the sum of all magnetic fields at point $P(x_i, y_i, z_i)$ due to each doublet,

$$h_i = \sum_{j=1}^{M} a_{ij} \cdot p_j \qquad \text{for } i = 1, 2, \ldots, N, \tag{4}$$

where N is the number of observations and M is the number of doublets.

The linear system of equations (4) can be written in matrix notation

$$\mathbf{h} = \mathbf{A}\mathbf{p}, \tag{5}$$

where $\mathbf{h}$ is the vector containing the computed magnetic field at the observation points due to a layer of doublets, $\mathbf{A}$ is a matrix whose a_{ij} element is given by equation (3), and $\mathbf{p}$ is the vector containing the doublet strengths.

Using the equivalent layer theorem, I approximate the observations by the magnetic field due to the equivalent layer

$$\mathbf{h}^0 = \mathbf{A}\mathbf{p}, \tag{6}$$

where $\mathbf{h}^0 = (h_1^0, h_2^0, \ldots, h_N^0)^T$ is the vector containing the observations.

The smaller the doublet length b relative to the sampling interval, the better the approximation by the equivalent sources. However, if the doublet length is too small relative to the sampling interval, matrix $\mathbf{A}$ becomes ill-conditioned because the coefficients a_{ij} in equation (3) tend to very small values. A value of b between one-half and one-fifth of the sampling interval was found to produce good results.

From equation (6) I obtain an estimate for $\mathbf{p}$

$$\mathbf{p}^* = \mathbf{A}^+ \mathbf{h}^0, \tag{7}$$

where $\mathbf{A}^+$ is a suitable pseudoinverse for $\mathbf{A}$.

Once the vector $\mathbf{p}$ of strengths is estimated, it is trivial to obtain the magnetic field reduced to the pole. The inclinations of the doublets and the geomagnetic field in equation (3) are changed to 90 degrees, obtaining

$$b_{ij} = \frac{z_i - d - \dfrac{b}{2}}{\left[(x_i - x_j')^2 + (y_i - y_j')^2 + \left(z_i - d - \dfrac{b}{2}\right)^2\right]^{3/2}}$$

$$-\frac{z_i - d + \dfrac{b}{2}}{\left[(x_i - x_j')^2 + (y_i - y_j')^2 + \left(z_i - d + \dfrac{b}{2}\right)^2\right]^{3/2}}, \tag{8}$$

and the total field at the pole is computed by

$$\mathbf{h}_{\text{pole}} = \mathbf{B}\mathbf{p}^*, \tag{9}$$

where $\mathbf{B}$ is a matrix whose b_{ij} element is given by equation (8).

Substituting equation (7) in equation (9),

$$\mathbf{h}_{\text{pole}} = \mathbf{B}\mathbf{A}^+\mathbf{h}^0, \tag{10}$$

or

$$\mathbf{h}^0 = \mathbf{A}\mathbf{B}^+\mathbf{h}_{\text{pole}}. \tag{11}$$

Equation (11) represents the formulation of reduction to the pole as an inverse problem. The system of linear equations (6) is ill-conditioned, i.e., large changes in the solution may result from small changes in the vector of observations. To find stable solutions to this system, I use the results given in Tikhonov and Arsenin (1977) and Hoerl and Kennard (1970a, b) and compute the stable least-squares solution to equation (6) by

$$\mathbf{p}^* = \mathbf{D}(\mathbf{D}\mathbf{A}^T\mathbf{A}\mathbf{D} + \lambda\mathbf{I})^{-1}\mathbf{D}\mathbf{A}^T\mathbf{h}^0, \tag{12}$$

where $\mathbf{D}$ is a diagonal scaling matrix with elements

$$d_{ii} = \frac{1}{\left(\sum_{j=1}^{N} a_{ji}^2\right)^{1/2}},$$

and λ is a real positive number usually, between 0 and 1. Criteria for selection of the best value of λ are given in Hoerl and Kennard (1970b).

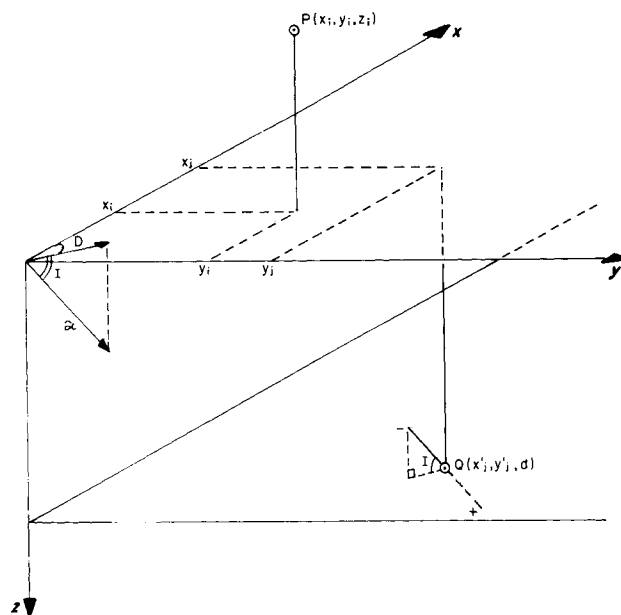Substituting equation (12) in equation (9),

FIG. 6. Position of the doublets with respect to the observations. All doublets are parallel to the direction of magnetization and their centers are on plane $z = d$.
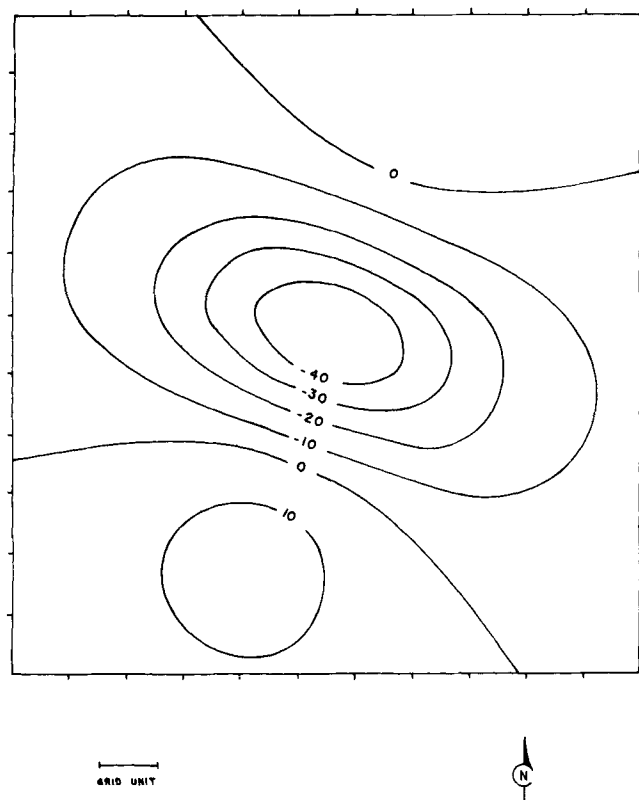
$$\mathbf{h}_{\text{pole}} = \mathbf{\underline{R}} \mathbf{h}^0, \tag{13}$$

where

$$\mathbf{\underline{R}} = \mathbf{\underline{B}} \mathbf{\underline{D}} (\mathbf{\underline{D}} \mathbf{\underline{A}}^T \mathbf{\underline{A}} \mathbf{\underline{D}} + \lambda \mathbf{\underline{I}})^{-1} \mathbf{\underline{D}} \mathbf{\underline{A}}^T. \tag{14}$$

Equation (13) allows the computation of stabilized reduced-to-the-pole fields by a suitable choice of λ. For fixed values of I, I_0, D, D_0, d, and λ, matrix $\mathbf{\underline{R}}$ has to be computed just once, and it may be stored in a suitable device for future use. In this case, the procedure becomes more efficient because the computation of $\mathbf{\underline{R}}$ accounts for more than 90 percent of the total processing time.

ANALYSIS OF THEORETICAL DATA

The proposed technique is now applied to theoretical data and the results are analyzed. To generate the vector of "observations" $\mathbf{h}^0$, I computed the total field due to the same prism shown in Figure 1 at discrete points on the plane $z = 0$ using a 12×12 square grid. The magnetization vector and the geomagnetic field have inclination of 5 degrees and azimuth of 20 degrees with respect to the x-axis. The magnetic field produced by this prism is shown in Figure 7. I analyze three cases: noise-free data, noise-corrupted data, and truncated anomaly. In all cases I used the same number of doublets as observations and the doublets were located directly below the observations.

FIG. 7. Total field produced by the basic prism shown in Figure 1. $I = I_0 = 5$ degrees and $D = D_0 = 20$ degrees. Contour intervals: 10 nT.
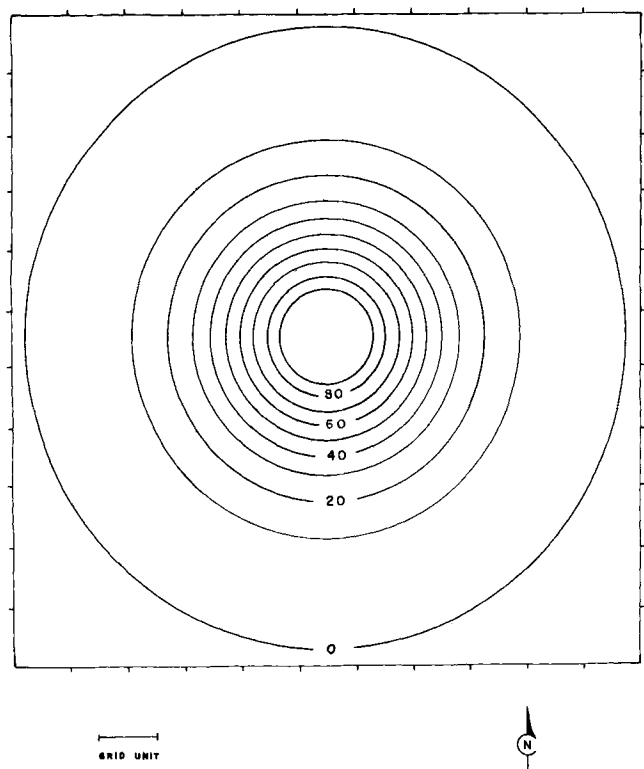
FIG. 8. Total field reduced to the pole obtained by the application of the proposed technique to the magnetic field shown in Figure 7 and employing $\lambda = 0$. Contour intervals: 10 nT.
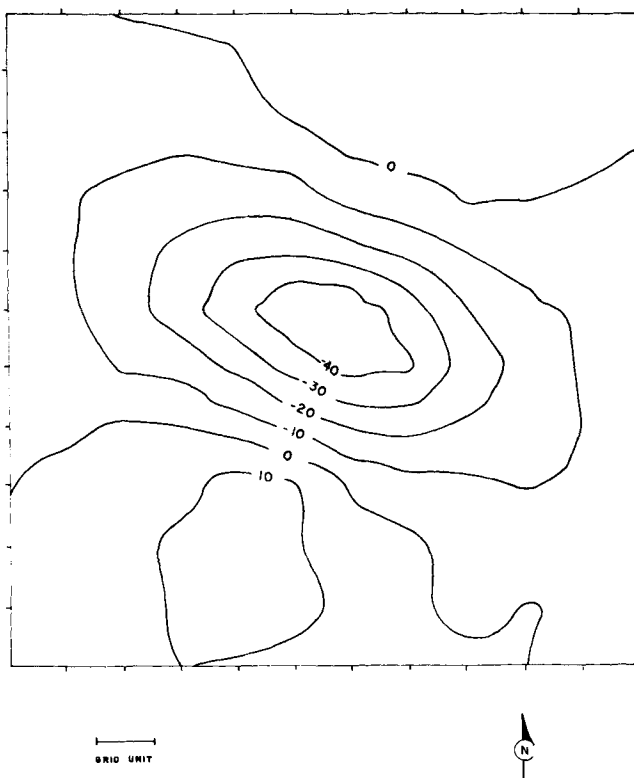

FIG. 9. Total field due to the basic prism and corrupted with additive, Gaussian noise having standard deviation of 1.6 nT. $I = I_0 = 5$ degrees and $D = D_0 = 20$ degrees. Contour intervals: 10 nT.

Noise-free data

Figure 8 shows the magnetic field reduced to the pole using equation (13). Because there is no noise in data, λ equals zero was assumed. Comparing Figures 1, 3, and 8, note that the proposed technique is not sensitive to the inclination of either the magnetization or the geomagnetic field. I tested the technique using several inclinations (including zero) and several azimuths with respect to the x-axis. The computed reduced-to-the-pole map remains virtually the same as the one shown in Figure 8.

Noise-corrupted data

Figure 9 represents the same field as in Figure 7 but corrupted with additive, zero-mean, Gaussian noise. The noise standard deviation is 1.6 nT, corresponding to 4 percent of the negative peak value.

Magnetic fields reduced to the pole are shown in Figures 10 and 11. In Figure 10 I used the FFT filtering technique, and in Figure 11 I used equation (13) with $\lambda = 0.001$. A criterion similar to the analysis of "ridge trace," proposed in Hoerl and Kennard (1970b), was employed to find the best value of λ.

Comparison of Figures 10 and 11 shows that, in contrast to FFT filtering, the proposed technique provides a valuable means of producing meaningful reduced-to-the-pole maps at low magnetic latitudes.

It should be pointed out that even though a stabilizing procedure for the FFT reduction to the pole has been suggested in Pearson and Skinner (1982), it consists of a filtering applied *to the data*, which presents two disadvantages. First, the procedure requires a priori information about the noise present in the data. Second, elimination of noise by spectral techniques is not perfect and it may incur elimination of part of the signal as well. On the other hand, formulating the problem of reduction to the pole as an inverse problem, the stabilization is applied *to the method*, leaving the data unaltered. Because the optimum stabilizing parameter can be determined by an objective criterion (Hoerl and Kennard, 1970b), it follows that no a priori knowledge about the noise is required.

Figure 12 shows the magnetic field of Figure 7 corrupted by Gaussian noise with standard deviation 8 nT which corresponds to 20 percent of the negative peak value. Figure 13 shows the magnetic field reduced to the pole using equation (13) with $\lambda = 0.01$. Despite the high noise level, the result shown in Figure 13 is still reasonable. The FFT filtering produces a totally meaningless map in this case.

For comparison, a test similar to the one just described was performed with $I = I_0 = 60$ degrees and $D = D_0 = 20$ degrees. The additive Gaussian noise has standard deviation 3.2 nT corresponding to 4 percent of the anomaly peak value. It was found that FFT filtering produces a satisfactory reduction to the pole, confirming that the instability of this technique occurs mainly at low latitudes.

Truncated anomaly

In practice, reduction to the pole is applied to areas of finite extent so that truncated anomalies may be expected at the borders, giving rise to undesirable edge effects. I show now that anomaly truncation at low magnetic latitudes does not appreciably affect the results obtained by the equivalent layer technique, but greatly accentuates the instability of FFT reduction to the pole.

Figure 14 shows the same anomaly as in Figure 1 but shifted four grid units in the positive x- and y-direction. The corresponding truncated anomaly for $I = I_0 = 5$ degrees and $D = D_0 = 20$ degrees was reduced to the pole first using the FFT filtering and then using equation (13) assuming $\lambda = 0$. The results are shown in Figures 15 and 16, respectively. Figure 15 shows that the anomaly is still undetected but the numerical values are totally unrealistic. Moreover, there is a noticeable spurious trend along 20 degrees northeast. A profile normal to this direction shows oscillations having a peak-to-peak amplitude of more than 300 nT. This amplitude is more than 3 times the amplitude of the true reduced-to-the-pole anomaly. On the other hand, Figure 16 shows that the proposed technique yields a stable solution to the problem, producing a map only slightly distorted as compared with the true magnetic field at the pole (Figure 14).

A test similar to the one described above was performed with $I = I_0 = 60$ degrees and $D = D_0 = 20$ degrees. The proposed technique produces a map that is virtually the same as the one in Figure 14. FFT filtering produces the map shown in Figure 17. Comparison of Figures 14 and 17 shows that even though the shape and position of the true anomaly at the pole are attained by FFT filtering, there is a distortion in the slope and amplitude of the filtered anomaly.

Results so far show that, in contrast to FFT filtering, the proposed technique provides excellent reduction-to-the-pole maps when theoretical data are used, because the equivalent layer technique does not use the Fourier spectrum. FFT filtering, on the other hand, uses the discrete Fourier spectrum which, even for theoretical data, contains imperfections caused by Gibbs' phenomenon and aliasing. Moreover, equation (2) shows that the reduction-to-the-pole filter presents numerical poles at $I = 0$ degrees or $I_0 = 0$ degrees which are responsible for the accentuated instability at low latitudes.

By contrast, the system of linear equations (6) is ill-conditioned at low magnetic latitudes, i.e., at least one of the singular values of A is very small, but still *different from zero* which accounts for the much better performance of the technique in contrast to FFT filtering *when "perfect" data are used*. In the presence of noise, both techniques yield unstable solutions and some stabilizing procedure must be applied. When working with an FFT filter, we obtain a more perfect representation of the Fourier spectrum either by using a larger gridding area (as shown in Figure 4) or by eliminating part of the high-frequency noise by a low-pass filter. Both alternatives present disadvantages. On the other hand, when using the equivalent-layer approach, well-known methods for computing stable solutions of a linear inverse problem can be used. At high magnetic latitudes both techniques are stable.

Restrictions on the depth of the equivalent layer

Dampney (1969) investigated the conditions under which the approximation of the continuous equivalent layer by a discrete layer remains valid for the gravimetric case. He concluded that the depth of the equivalent layer must be between 2.5 and 6 times the grid spacing.

My tests indicate the limits on the depth of the equivalent layer are about the same as those found by Dampney (1969). The lower limit follows from the fact that the approximation
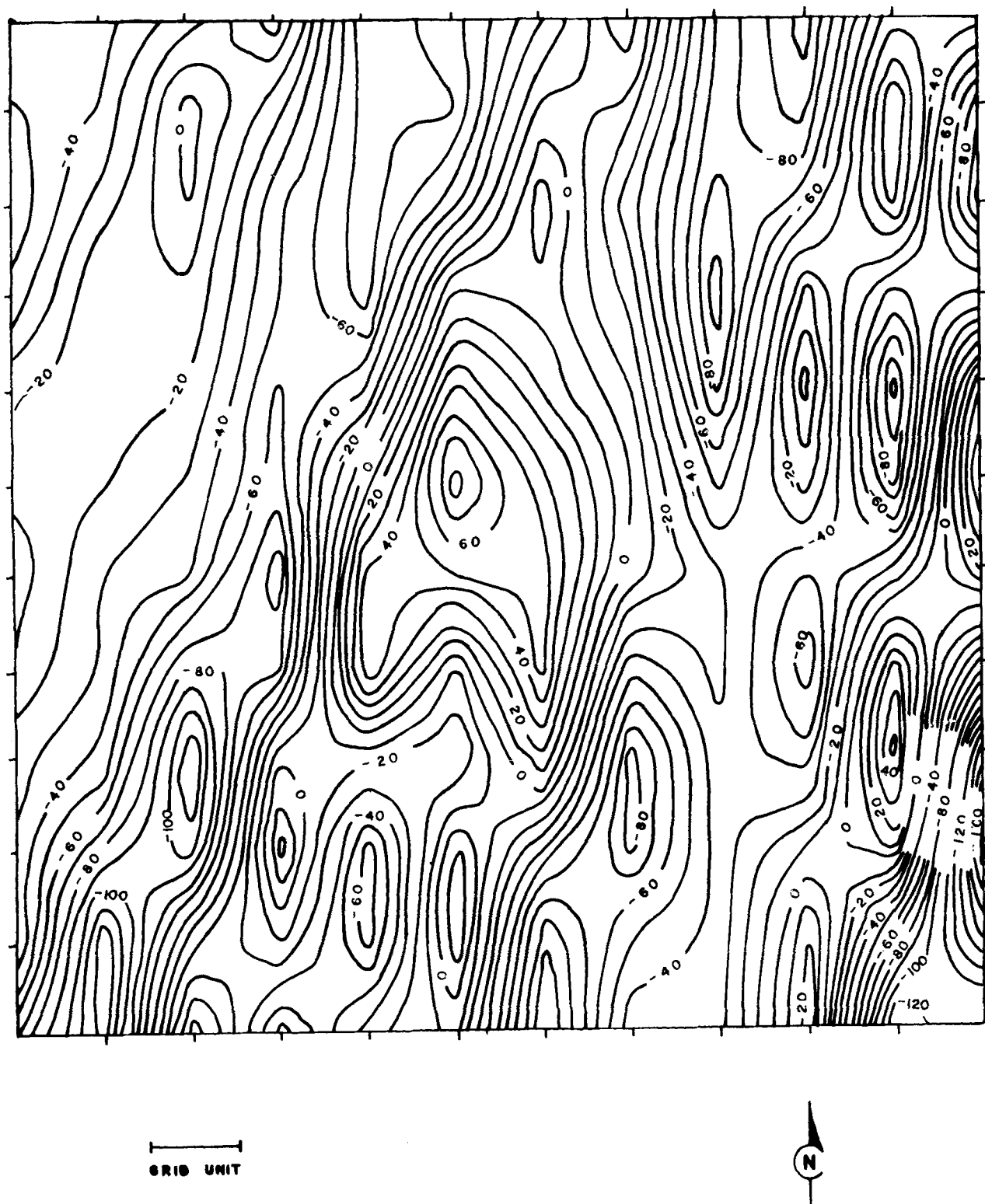
Fig. 10. Total field reduced to the pole obtained by FFT filtering applied to the noise-corrupted field shown in Figure 9. Contour intervals: 10 nT.
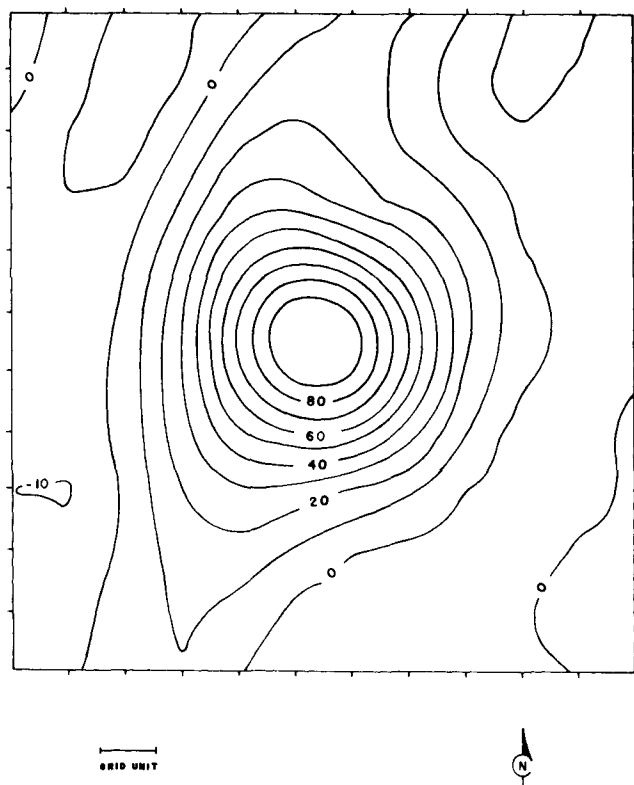
FIG. 11. Total field reduced to the pole obtained by application of the proposed technique to the magnetic field shown in Figure 9 and employing $\lambda = 0.001$. Contour intervals: 10 nT.
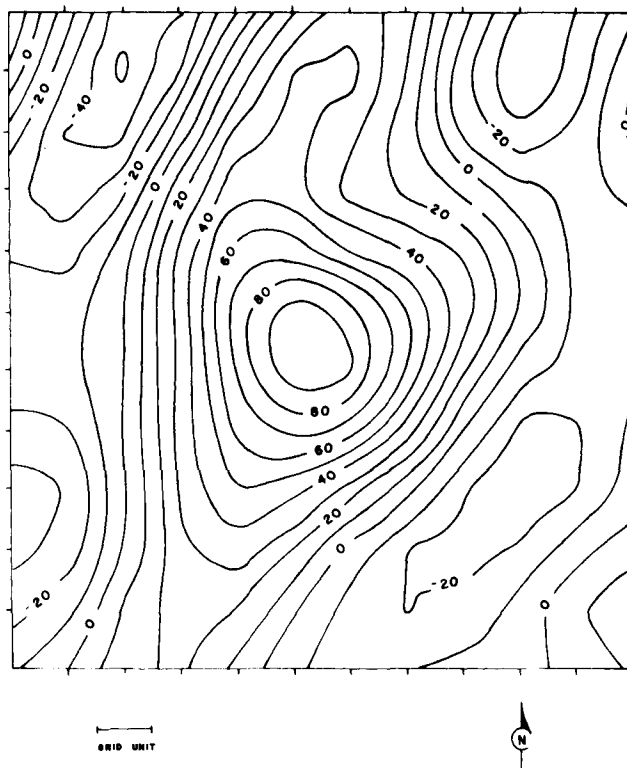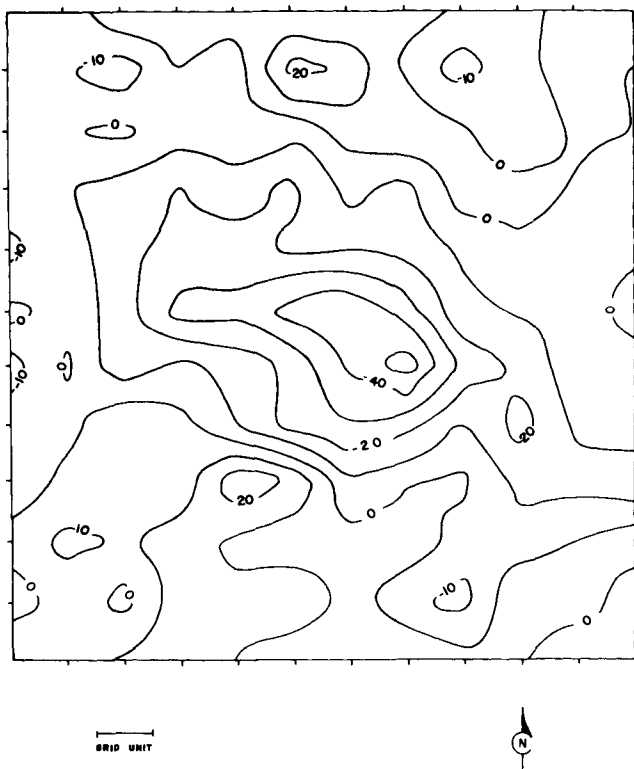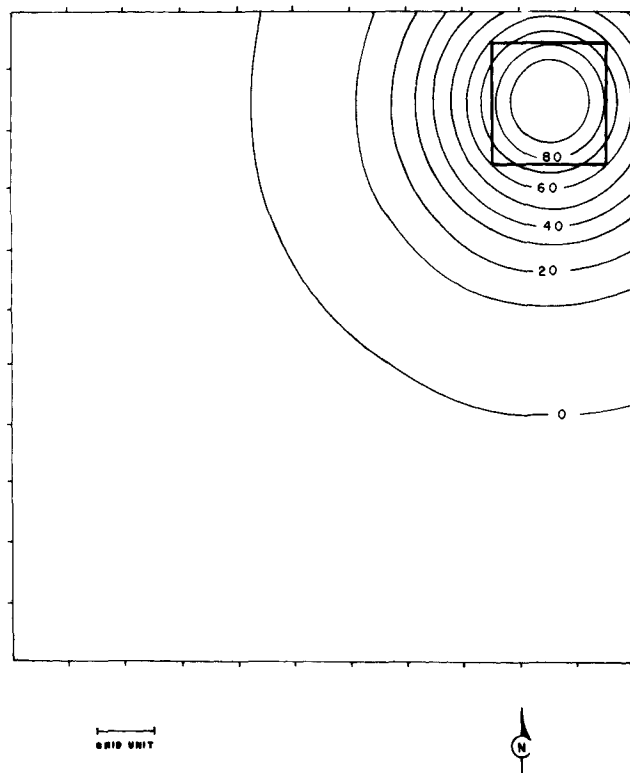

FIG. 13. Total field reduced to the pole obtained by application of the proposed technique to the magnetic field shown in Figure 12 and employing $\lambda = 0.01$. Contour intervals: 10 nT.

FIG. 12. Total field due to the basic prism and corrupted with additive, Gaussian noise having standard deviation of 8 nT. $I = I_0 = 5$ degrees and $D = D_0 = 20$ degrees. Contour intervals: 10 nT.

FIG. 14. Plan view of the basic model and its truncated theoretical total field anomaly at pole. Contour intervals: 10 nT.
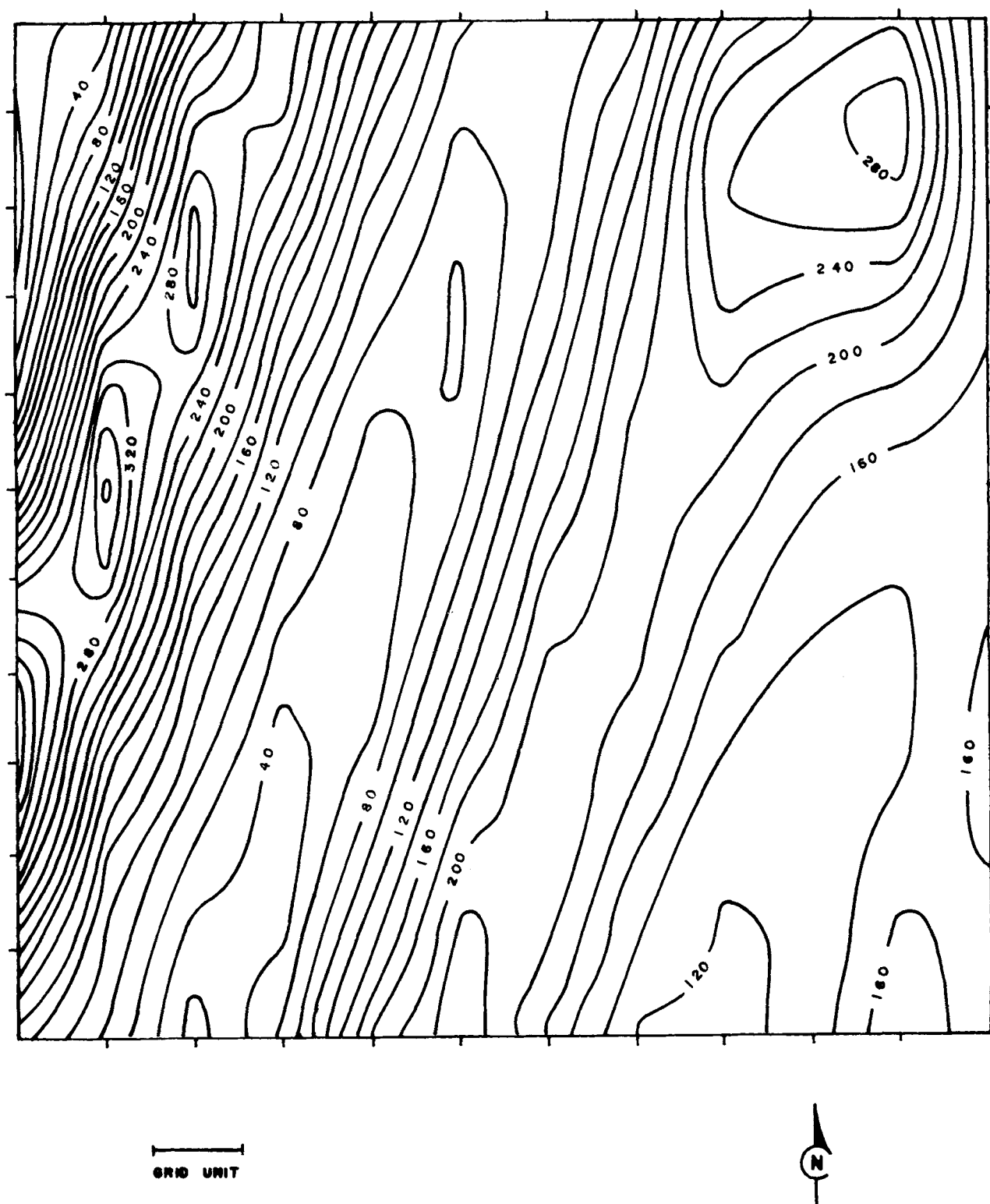
FIG. 15. Total field reduced to the pole obtained by FFT filtering applied to the truncated anomaly due to the prism shown in Figure 14 with $I = I_0 = 5$ degrees and $D = D_0 = 20$ degrees. Contour intervals: 10 nT.

of the discrete doublets to a continous distribution of magnetization produces a valid representation of the magnetic field **h** if the doublets are sufficiently far from the surface of measurements relative to the average doublet spacing. The upper limit follows from the fact that the elements of matrix A [equation (3)] approach a common value when d is large relative to the doublet spacing, causing the system to be ill-conditioned [equation (6)]. Also, to improve the performance of the proposed technique, the average spacing employed for the observations must be at most one-half the depth to the top of the sources because a sample spacing more than one-half the depth to the top of the sources yields a poor representation of the magnetic field.

In summary, the restriction on the use of the proposed technique is that the discretization of both the (equivalent) sources and the observations should produce a valid representation of the observed magnetic field. Also, ill-conditioning should be avoided by a suitable choice of the depth of the equivalent layer.

APPLICATIONS TO REAL ANOMALIES

Gulf of Guinea

Figure 18 shows the total intensity field over a seamount in the Gulf of Guinea (Harrison, 1971). The bathymetric contours of the seamount are shown in Figure 19 in full lines.

Harrison (1971) interpreted the magnetic data using the method of Talwani (1965) and found as acceptable a seamount

with a nonmagnetic top (2.65–3.15 km) and with a uniformly magnetized bottom ($I = 23.9$ degrees and $D = 143.5$ degrees) extending below the ocean floor. Figure 19 shows in dashed lines the subbottom structure postulated in Harrison (1971).

Emilia and Massey (1974) interpreted the same anomaly assuming as a model for the seamount a set of rectangular prisms; each had a distinctive magnetization amplitude but they had a common magnetization direction. Their results were not significantly different from those obtained by Harrison: a nonmagnetic top with a magnetized bottom extending beneath the ocean floor. The magnetization direction is also similar, $I = 26.5$ degrees and $D = 142.0$ degrees.

To apply the proposed technique to this anomaly, the total field map of Figure 18 was digitized by hand in a 17 × 17 grid at intervals of 1.51 km in the x- and y-directions. A 17 × 17 discrete equivalent layer was employed where the doublets are centered directly below the observations. Figure 20 shows the reduced-to-the-pole anomaly using equivalent sources with $\lambda = 0.02$. The direction of magnetization was assumed to be the one given in Harrison (1971). Some important features are apparent in Figure 20. A single magnetic high having an amplitude of about 900 nT is located above the seamount. Also, the peak of the reduced-to-the-pole anomaly is very close to the top of the seamount (located at the origin of the x- and y-coordinates). Finally, the slightly regular shape of the western border of the seamount (Figure 19) is clearly revealed in the reduced-to-the-pole anomaly, and the negative contours at the top of Figure 19 probably reflect the shape of the northern border of the seamount.
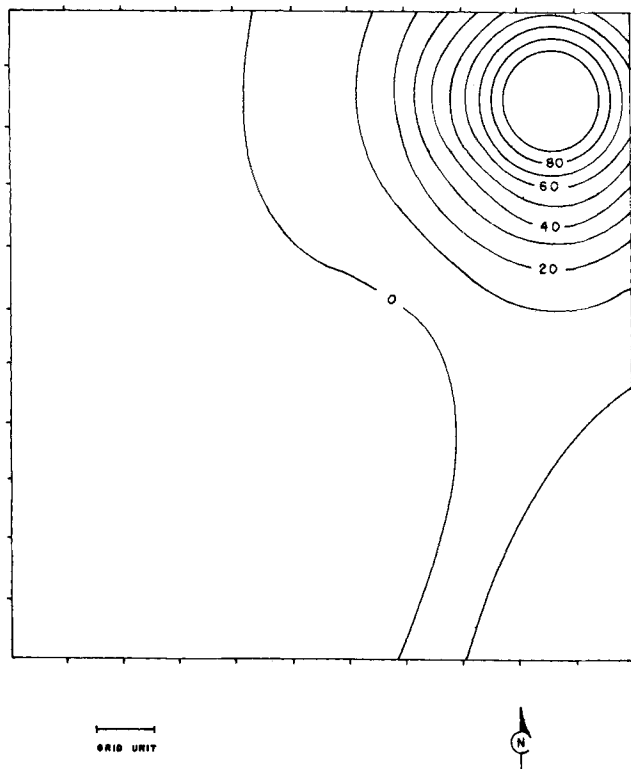

FIG. 16. Total field reduced to the pole obtained by application of the proposed technique to the truncated anomaly due to the prism shown in Figure 14 with $I = I_0 = 5$ degrees and $D = D_0 = 20$ degrees. Contour intervals: 10 nT.
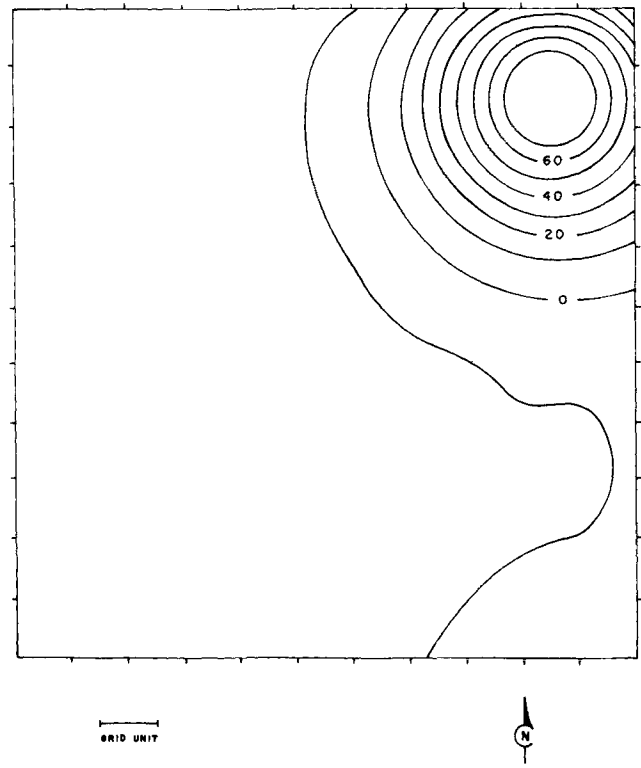
FIG. 17. Total field reduced to the pole obtained by FFT filtering applied to the truncated anomaly due to the prism shown in Figure 14 with $I = I_0 = 60$ degrees and $D = D_0 = 20$ degrees. Contour intervals: 10 nT.

Parnaiba basin, Brazil

Figure 21 shows the total intensity aeromagnetic map (DNPM, 1979) from a survey flown in 1976 over a portion of the western border of the Parnaiba Basin, Brazil. Figure 22 shows a geologic map of the area (Silva and Sá, 1982). This basin consists of 2 500 to 3 000 m of Paleozoic and Mesozoic sedimentary rocks, mainly conglomerates, sandstones, shales, siltstones, limestones, and marls. To the west, the Parnaiba Basin is limited by the Paraguai-Araguaia Orogenic Belt consisting of Precambrian metasedimentary rocks and mafic and ultramafic intrusive rocks. Part of the Paraguai-Araguaia Orogenic Belt is buried by the sedimentary rocks of the Parnaiba Basin.

The magnetic anomalies observed over the western border of Parnaiba Basin may be due to two distinct types of sources: either dikes and flows of basaltic rocks representing the extensive volcanism that took place at the end of the Jurassic period, or deep-seated mafic and ultramafic intrusions in the basement (possibly representing buried portions of the orogenic belt). The magnetic anomaly of Figure 21 is caused by sources of the second type.

The total field map of Figure 21 was digitized by hand using a 16×16 grid at intervals of 700 m in the x- and y-directions corresponding to north-south and east-west directions, respectively. The local geomagnetic field in 1976 had inclination of -1.4 degrees and declination of -16.42 degrees. Induced magnetization was assumed for the source.

The anomaly was reduced to the pole first using FFT filter-ing over the 16×16 gridding area, and then using the equivalent-layer technique over a 12×12 gridding area with $\lambda = 0.06$ and employing a discrete 12×12 equivalent layer with doublets centered directly below the observations. The results are shown in Figures 23 and 24, respectively. As expected, the FFT filtering produced an unstable solution denoted by the accentuated high-amplitude oscillations in the direction perpendicular to the geomagnetic field. On the other hand, the equivalent-layer technique produced a stable and meaningful reduced-to-the-pole map, displaying a single positive anomaly with an amplitude of about 80 nT.

CONCLUSIONS

I analyzed a technique for reducing magnetic anomalies to the pole using equivalent sources. The technique produces stable transformations at any latitude and also in the presence of noise, so I propose it as an alternative to the traditional FFT filtering. Using theoretical data, a comparison is made between the traditional FFT filtering and the proposed technique. The results indicate that, in general, at high latitudes both techniques yield the same results except when the anomaly is truncated. In this case, the proposed technique produces the best results. At low magnetic latitudes (less than 15 degrees) the FFT technique has a poor performance, particularly in the presence of noise. By contrast, the proposed technique is less sensitive to the magnetic inclination and produces meaningful results even in the presence of noise. It should be pointed out that in the tests using theoretical data, the proposed
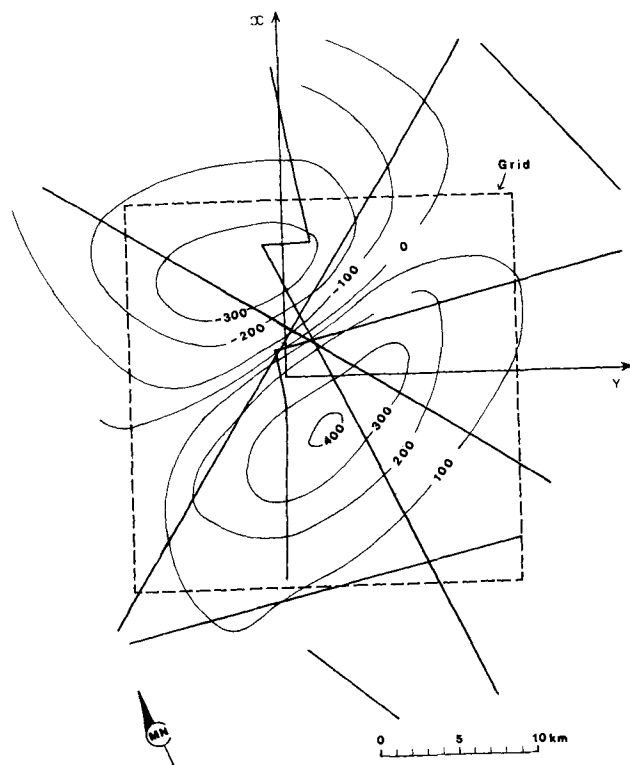

Fig. 18. Magnetic anomaly map of the Gulf of Guinea seamount and the reference system employed. Thick lines are the ship tracks. Contour intervals: 100 nT.
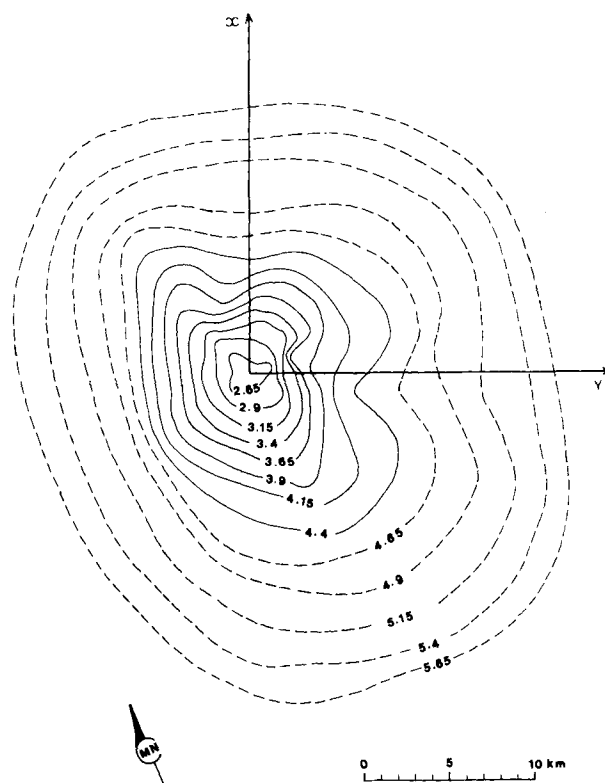

Fig. 19. Bathymetric contour map of the Gulf of Guinea seamount. Contour intervals: 0.25 km. The seamount is centered at 0°23′N, 2°38′E. MN is magnetic north and the dashed contours represent the subbottom structure postulated in Harrison (1971).
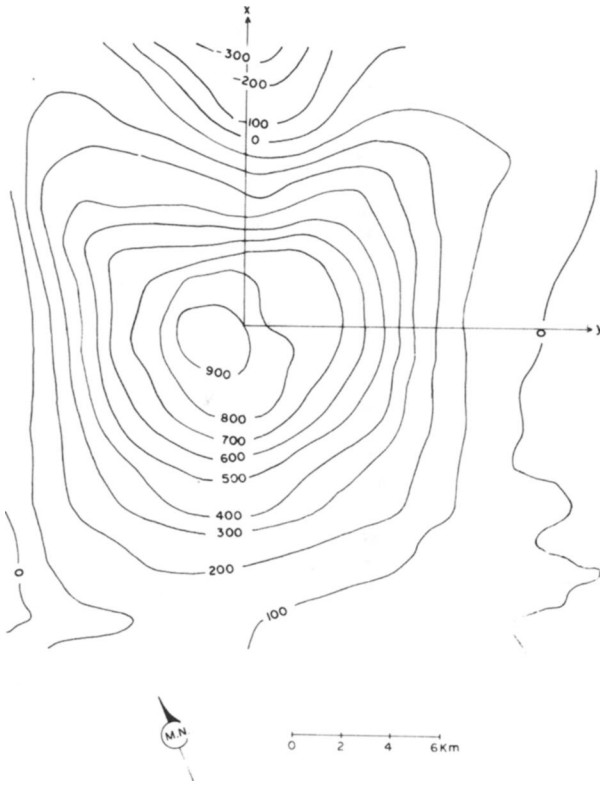
FIG. 20. Magnetic anomaly map of the Gulf of Guinea seamount reduced to the pole by the equivalent source technique with $\lambda = 0.02$. Contour intervals: 100 nT.
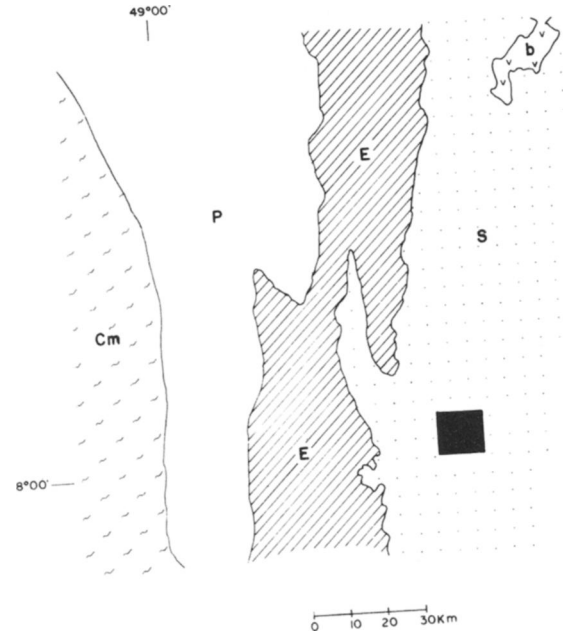

FIG. 22. Geologic map of the western border of Parnaiba Basin (Silva and Sá, 1982). The black square indicates the area of the magnetic anomaly map shown in Figure 21. S and b are sedimentary rocks and basalts, respectively, from Parnaiba Basin. The Paraguai-Araguaia Orogenic Belt comprises the Couto Magalhães (Cm) and Pequizeiro (P) formations, and the Estrondo group (E).
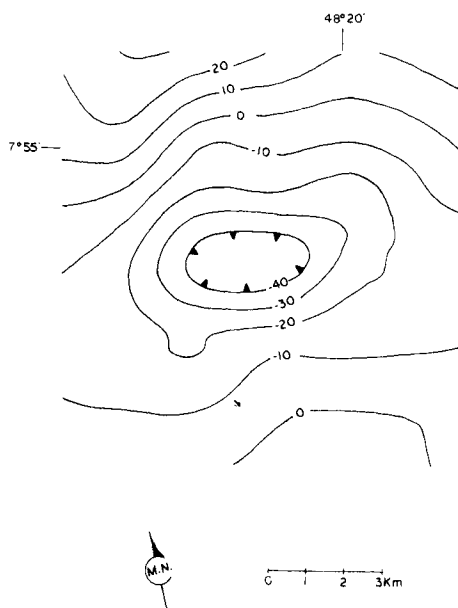

FIG. 21. Magnetic anomaly map of the Parnaiba Basin area. Contour intervals: 10 nT.
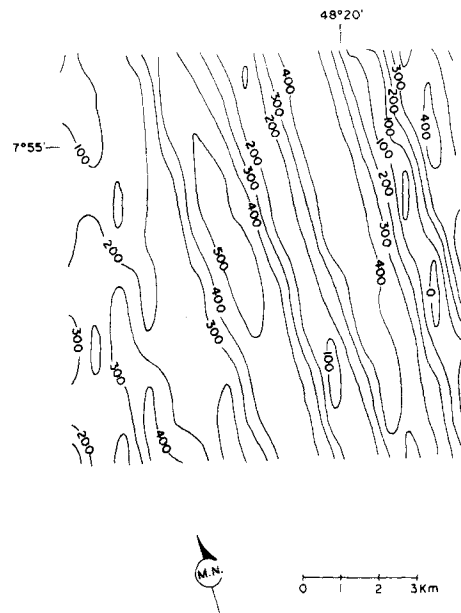

FIG. 23. Magnetic anomaly map of the Parnaiba Basin area reduced to the pole by FFT filtering. Contour intervals: 10 nT.

technique always performed better than the FFT technique despite the smaller 12 × 12 gridding area employed, as compared with the 16 × 16 gridding area employed in the FFT filtering.

Another advantage of the proposed technique is that the base level of the reduced-to-the-pole anomaly is not undefined as is the case with FFT filtering.

The proposed technique was applied to two actual low-latitude anomalies. In both cases it proved useful in removing the severe distortion caused by the low magnetic inclination. The conclusions obtained from the analysis of theoretical anomalies were confirmed in both areas.

Among the restrictions to application of the proposed technique are the constraints in the range of the equivalent layer depth and the depth to the top of the sources in terms of the grid units (in the case of a regular grid) employed for the observations and doublets. The grid unit for the observations should be at most one-half the depth to the top of the sources and the equivalent layer should be at a depth between 2 and 6 grid units employed for the doublets.

Although the proposed technique requires 50 times more processing time than that for FFT filtering, the absolute time necessary is still modest. To process a 12 × 12 array on a DEC-10 computer takes about 45 s. Moreover, when using a regular grid, processing time can be reduced by more than 90 percent if matrix $\mathbf{R}$ in equation (14) is computed beforehand for fixed values of I, I_0, D, D_0, d, and λ and stored. As a result, very large areas can be processed by a piece-wise application of equation (13), i.e., moving the operator $\mathbf{R}$ around until the entire map is processed. Edge effects can be minimized by overlapping adjacent areas, discarding some values at the borders, and choosing λ carefully.

REFERENCES

Baranov, V., 1957, A new method for interpretation of aeromagnetic maps: Pseudo-gravimetric anomalies: Geophysics, **22**, 359–383.
Baranov, V., and Naudy, H., 1964, Numerical calculation of the formula of reduction to the magnetic pole: Geophysics, **29**, 67–79.
Bhattacharyya, B. K., 1964, Magnetic anomalies due to prism-shaped bodies with arbitrary polarization: Geophysics, **29**, 517–531.
——— 1965, Two-dimensional harmonic analysis as a tool for magnetic interpretation: Geophysics, **30**, 829–857.
Bott, M. H. P., and Ingles, A., 1972, Matrix method for joint interpretation of two-dimensional gravity and magnetic anomalies with application to the Iceland-Faeroe Ridge: Geophys. J. Roy. Astr. Soc., **30**, 55–67.
Dampney, C. N. G., 1969, The equivalent source technique: Geophysics, **34**, 39–53.
DNPM, 1979, Projeto geofísico Brasil-Canadá: mapa de intensidade magnética total, folha SB.22-Z-D-VII: Geophysical project Brazil-Canada: total intensity magnetic map, sheet SB.22-Z-D-VII.
Emilia, D. A., 1973, Equivalent sources used as an analytic base for processing total magnetic field profiles: Geophysics, **38**, 339–348.
Emilia, D. A., and Massey, R. L., 1974, Magnetization estimation for nonuniformly magnetized seamounts: Geophysics, **39**, 223–231.
Ervin, C. P., 1976, Reduction to the magnetic pole using a fast Fourier series algorithm: Computers and Geosciences, **2**, 211–217.
Gunn, P. J., 1975, Linear transformations of gravity and magnetic fields: Geophys. Prosp., **23**, 300–312.
Harrison, C. G. A., 1971, A seamount with a nonmagnetic top: Geophysics, **36**, 349–357.
Hinze, W. J., von Frese, R. R. B., Longacre, M. B., Braile, L. W., Lidiak, E. G., and Keller, G. R., 1982, Regional magnetic and gravity anomalies of South America: Geophys. Res. Lett., **9**, 314–317.
Hoerl, A. E., and Kennard, R. W., 1970a, Ridge regression: biased estimation for nonorthogonal problems: Technometrics, **12**, 55–67.
——— 1970b, Ridge regression: Applications to nonorthogonal problems: Technometr., **12**, 69–82.
Kanasewich, E. R., and Agarwal, R. G., 1970, Analysis of combined gravity and magnetic fields in wavenumber domain: J. Geophys. Res., **75**, 5702–5712.
Langel, R. A., Slud, E. V., and Smith, P. J., 1984, Reduction of satellite magnetic anomaly data: J. Geophys., **54**, 207–212.
Mayhew, M. A., 1979, Inversion of satellite magnetic anomaly data: J. Geophys., **45**, 119–128.
——— 1982, An equivalent layer magnetization model for the United States derived from satellite altitude magnetic anomalies: J. Geophys. Res., **87**, 4837–4845.
Mayhew, M. A., Johnsen, B. D., and Langel, R. A., 1980, An equivalent source model of the satellite-altitude magnetic anomaly field over Australia: Earth Plan. Sci. Lett., **51**, 189–198.
Pearson, W. C., and Skinner, C. M., 1982, Reduction-to-the-pole of low-latitude magnetic anomalies: Presented at the 52nd Ann. Internat. Mtg. and Expos., Soc. Explor. Geophys.
Roy, A., 1962, Ambiguity in geophysical interpretation: Geophysics, **27**, 90–99.
Silva, R. W. S., and Sá, J. H. S., 1982, Feições geológicas e magnetométricas da região do baixo Araguaia: Anais do primeiro simpósio de geologia da Amazônia, **1**, 259–269.
Talwani, M., 1965, Computation with the help of a digital computer of magnetic anomalies caused by bodies of arbitrary shape: Geophysics, **30**, 797–817.
Tikhonov, A. N., and Arsenin, V. Y., 1977, Solutions to ill-posed problems: V. H. Winston & Sons.
von Frese, R. R. B., Hinze, W. J., and Braile, L. W., 1981, Spherical earth gravity and magnetic anomaly analysis by equivalent point source inversion: Earth Plan. Sci. Lett., **53**, 69–83.
——— 1982, Regional North American gravity and magnetic anomaly correlations: Geophys. J. Roy. Astr. Soc., **69**, 745–761.
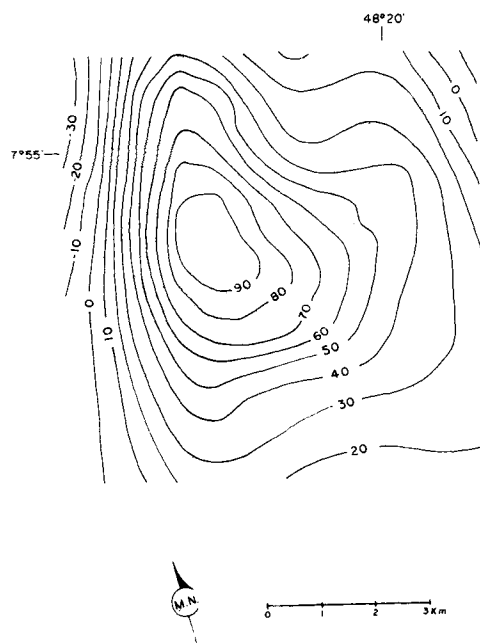

FIG. 24. Magnetic anomaly map of the Parnaiba Basin area reduced to the pole by the equivalent layer technique with $\lambda = 0.06$. Contour intervals: 10 nT.